Vol. 79: 207–218, 2020
https://doi.org/10.3354/cr01592

CLIMATE RESEARCH
Clim Res

Published online March 26

Reconstructing summer upper-level flow in the northern Rocky Mountains using an alpine larch tree-ring chronology

Evan E. Montpellier[1,*], Peter T. Soulé[1], Paul A. Knapp[2], L. Baker Perry[1]

[1]Department of Geography and Planning, Appalachian State University, Boone, NC 28608, USA
[2]Department of Geography, Environment, and Sustainability, University of North Carolina at Greensboro, Greensboro, NC 27412, USA

ABSTRACT: Mid-latitude mesoscale weather during the climatological summer is strongly influenced by fluctuations in synoptic-scale circulation patterns. Previous research has linked Arctic amplification to alterations in summer synoptic climatology, leading to more extreme weather events in the mid-latitudes. In this study, seasonal (JJA) upper-level (500 hPa) atmospheric flow is reconstructed in the mid-latitudes using an alpine larch *Larix lyallii* Parl. tree-ring chronology sampled from western Montana. Significant relationships were found between alpine larch radial growth and upper-level flow patterns derived from the North American Regional Reanalysis dataset (1979–2015). Meridional and zonal flows that manifest in ridging are associated with enhanced radial growth of alpine larch (i.e. meridional flow west [$r = 0.504$, $p = 0.001$] and zonal flow north [$r = 0.642$, $p < 0.001$] of the study site). Meridional and zonal flows associated with troughing result in decreased radial growth (i.e. meridional flow east [$r = -0.497$, $p = 0.001$] and zonal flow south [$r = -0.584$, $p < 0.001$] of the study site). Using the leave-one-out method, a linear regression model was calibrated and verified between a principal component analysis score derived from measurements of upper-level flow in western North America and alpine larch tree growth. The 444 yr climate reconstruction of summer 500 hPa flow suggests that ridging is becoming more intense over the western United States and Canada since the 1980s.

KEY WORDS: Dendroclimatology · *Larix lyallii* · Climate reconstruction · Atmospheric flow · Synoptic climatology

1. INTRODUCTION

Variability in synoptic-scale circulation influences mesoscale meteorology during the climatological summer in the mid-latitudes, as the strength and amplitude of meridional and zonal flows largely dictate surface weather conditions. Several studies (Francis & Vavrus 2012, Porter et al. 2012, Screen & Simmonds 2013, Wu & Smith 2016, Francis 2017, Vavrus et al. 2017) have documented changes in upper-level atmospheric flow associated with Arctic amplification (AA), defined as the disproportionate heating of the high northern latitudes compared to the rest of the Northern Hemisphere (Francis & Vavrus 2012). Francis & Vavrus (2012) suggest that modified upper-level flow resulting from AA will lead to more extreme weather events in the mid-latitudes, specifically heat-related extremes. These atypical and extreme events carry negative implications for the built and natural environment and have the potential to affect millions of people living in the mid-latitudes through the increased frequency of drought (Cvijanovic et al. 2017, Vavrus et al. 2017), heat waves (Meehl & Tebaldi 2004, Tang et al. 2014, Vavrus et al. 2017), wildland fires (Knapp & Soulé 2017), and flooding (Francis & Vavrus 2012). Under-

Corresponding author: montp020@umn.edu

standing the temporal trends in upper-level flow based on proxy data helps place the current changes in mid-latitude synoptic-scale summer circulation in a historical context. Here we (1) demonstrate how upper-level (500 hPa) zonal and meridional winds spatially relate to radial tree growth at high elevations in the northern Rockies, (2) use a multi-century record of standardized radial tree growth to reconstruct a principal component-based measure of wind at 500 hPa over western North America, and (3) assess how upper-level flow has fluctuated spatiotemporally.

AA comprises most of the recent research surrounding mid-latitude summer synoptic climatology (e.g. Francis & Vavrus 2012, Cohen et al. 2014, Screen & Simmonds 2014, Tang et al. 2014). These studies assess the temporal attributes of upper-level atmospheric flow, yet most are limited in temporal resolution, as they rely heavily on the ERA-Interim reanalysis dataset (1979–present) and the NCEP–NCAR dataset (1948–present). Francis & Vavrus (2012) used the NCEP–NCAR reanalysis dataset to study the relationships between AA and the polar front jet stream and the associated climatic conditions in the mid-latitudes and found that (1) 1000–500 hPa thickness is reduced and (2) 500 hPa ridge peaks are becoming elongated. The implication of a reduction in 1000–500 hPa thickness is weaker zonal flow and therefore a slower progression of weather events. A more elongated ridge further amplifies the slower progression of weather events (Cohen et al. 2014). Screen & Simmonds (2014) and Tang et al. (2014), who use the ERA-Interim reanalysis dataset in their analysis, support the claim that AA has led to the slower progression of weather patterns and more weather extremes in the mid-latitudes. However, Barnes & Screen (2015) suggest that weakening and elongation of meridional flow are an artifact of the methodologies rather than true changes in mid-latitude summer synoptic climatology.

In an effort to extend the temporal record of mid- and upper-level flows, tree-ring data have been used as successful proxies to reconstruct jet stream flow in the Northern Hemisphere. Trouet et al. (2018) reconstructed latitudinal positioning of the North Atlantic Jet to AD 1725 in Europe using tree-ring records from the British Isles and northeastern Mediterranean. They found significant anomalous changes in the latitudinal positioning of the North Atlantic Jet that led to heat waves, droughts, and increased wildfire activity in Europe. Wise & Dannenberg (2014) reconstructed cool-season pressure patterns over North America using a network of tree-ring chronologies and found pronounced periods of persistent cool-season pressure patterns resulting in historic drought and pluvial periods. Seim et al. (2018) provide evidence that reconstructing large-scale atmospheric flow from tree-ring chronologies is a viable way to assess anthropogenic influences in atmospheric circulation and enables climate models to be improved. Others (e.g. Nichols et al. 1978, Casty et al. 2005, Wise & Dannenberg 2017) have reconstructed aspects of synoptic climatology in relation to fluctuations in upper-level flow in the mid-latitudes, but we find that a temporally robust record of upper-level flow for North American mid-latitude summers is lacking. Our study provides a historical perspective of upper-level (500 hPa) atmospheric flow in North America, specifically the western United States and southwestern Canada.

2. METHODS

2.1. Study Area

Alpine larch *Larix lyallii* Parl. (hereafter LALY) is a deciduous conifer endemic to the timberline zones (i.e. above ~2300 m) of the northern Rocky Mountains and responds positively to summer temperature (Arno & Habeck 1972, Graumlich & Brubaker 1986, Peterson & Peterson 1994, Kipfmueller 2008, Montpellier et al. 2018). LALY are predominantly found on cold, rocky sites with northern aspects and rarely occupy southern aspects (Arno & Habeck 1972). LALY growth occurs when mean temperatures are consistently above 5.6°C, which is approximately a 90 d growing season (Arno & Habeck 1972). Moisture is rarely a limiting factor in the growth of these trees, as they typically grow in cool, moist, and acidic soils (Arno & Habeck 1972). LALY are long-lived, with an average lifespan of 500 yr (Arno & Habeck 1972). In the northern Rockies of Montana, Kipfmueller (2008) found LALY dating back to AD 12 and successfully crossdated samples (expressed population signal [EPS] > 0.85; Wigley et al. 1984) over 1950 yr old for use in a summer temperature reconstruction. Thus, LALY can provide a useful proxy measurement of climatic conditions for multiple centuries.

2.2. Field Sampling

We collected LALY samples from 4 study site locations (Carlton Ridge, McCalla Lake, Sapphire Ridge, and Trapper Peak) located in the Bitterroot National

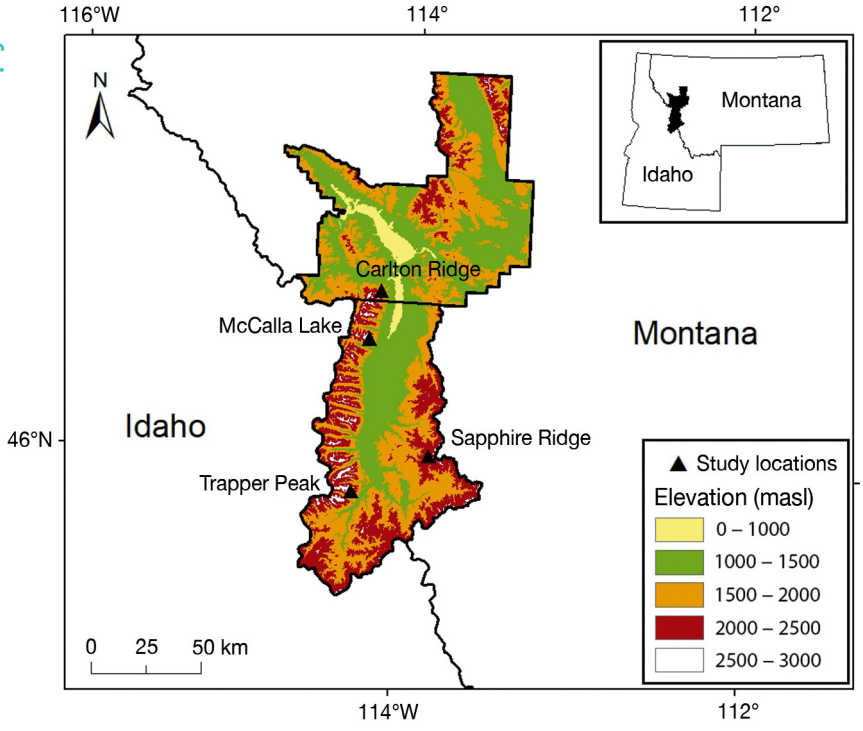

Fig. 1. Study sites in the Bitterroot National Forest of western Montana, USA. The boundaries of Missoula (north) and Ravalli (south) counties are shown

Forest (BNF) in western Montana (Fig. 1). Study site elevations ranged from 2400 to 2800 m. At nearby Missoula (elevation = 978.1 m), temperatures range from −5.0°C in January to 19.8°C in July, and the average annual precipitation is 34.5 cm (National Climatic Data Center 2016).

At each study site, we extracted a minimum of 2 core samples per tree using a 5.15 mm diameter increment borer from a minimum of 30 trees chosen via selective sampling. We sampled at breast height and perpendicular to the downward slope to avoid ring pinching. We avoided sampling trees with visible damage (e.g. bore damage, lightning scars, fire scars) and trees growing within a closed canopy (i.e. overlapping limbs).

2.3. Laboratory and Statistical Procedures

We sanded the core samples using progressively finer grit sandpaper (100–400 µm) to reveal cellular structure. We microscopically examined all cores and assigned a calendar year for each annual ring on each sample to crossdate the chronology (Stokes & Smiley 1996). We evaluated crossdating accuracy using the program COFECHA (Holmes 1983), and date adjustments (i.e. addressing missing rings) were made to cores that were flagged to correct errors. We used WinDENDRO (Regent Instruments 2011) to measure ring width to 0.001 mm precision.

We used the program ARSTAN (Cook 1985) to individually standardize the 152 core samples collected from the 4 study locations using the negative exponential curve option. We found that the strongest climate–growth relationships were obtained using a negative exponential detrending method and the standard chronology (Cook 1985). Individually, the 4 chronologies have strong interseries correlations and are moderately sensitive (Table 1). We assessed the relationship between each core and 500 hPa monthly zonal and meridional gridded (32 km) wind values (m s^{-1}) from the North American Regional Reanalysis (NARR) dataset (1979–2015; Mesinger et al. 2006) using Pearson correlation across the entire study region (25°–65° N, 90°–140° W). The NARR dataset is collected at 0.3° increments across North America. In an effort to reduce the number of variables in our field of study, we resampled our data by selecting the 500 hPa flow variable that was nearest to our 2.5° grid point. Although limited in temporal resolution, we elected to use the NARR dataset because of the enhanced data quality (i.e. more accurate wind, temperature, and precipitation measurements) when compared to other reanalysis datasets (Mesinger et al. 2006). The strongest relationships between radial growth and both zonal and meridional wind values occurred during summer (mean of JJA), so we used JJA for a more focused analysis

Table 1. Descriptive chronology statistics for the 4 study locations and a subset of the core samples (COMBO) in the Bitterroot National Forest in western Montana. Tree and core sample sizes only include trees and cores included in the final chronologies

Study location	Tree/core sample size	Mean sensitivity	Interseries correlation	Temporal resolution
Carlton Ridge	28/57	0.309	0.693	1580–2015
McCalla Lake	13/22	0.314	0.667	1685–2015
Sapphire Ridge	18/31	0.293	0.620	1730–2015
Trapper Peak	22/42	0.328	0.651	1538–2015
COMBO	27/37	0.314	0.689	1571–2015

using a subset of core samples (n = 37; hereafter COMBO). The cores excluded from COMBO were collected from southern aspects where climatic conditions, especially summer temperature, are moderated by increased insolation. Montpellier et al. (2018) report that LALY growing on non-southerly aspects better record changes in summertime ambient air temperature and that the primary control of summer temperature in the region is the upper-level flow regime (e.g. persistent ridging produces positive temperature anomalies) (Meehl & Tebaldi 2004, Screen & Simmonds 2014, Brewer & Mass 2017, Knapp & Soulé 2017). Thus, while all the trees we sampled across the 4 study sites have radial growth that is positively associated with surface temperature patterns controlled by upper-level atmospheric flow, the subset of cores we included in COMBO offers a more sensitive proxy for changes in 500 hPa flow. COMBO had an interseries correlation of 0.689, a mean sensitivity of 0.314, and an EPS of >0.85 during AD 1571–2015.

2.4. Climate Reconstruction and Verification Analysis

We used Pearson correlation to examine the relationships between 500 hPa zonal flow and 500 hPa meridional flow and tree growth (COMBO) at 378 grid point locations between 25°–65° N and 90°–140° W. We identified 2 broad areas of positive relationships between tree growth and 500 hPa flow located north and west of our study region, representing zonal wind (north) and meridional wind (west). We found 2 broad areas of negative relationships with 500 hPa flow south (zonal flow) and east (meridional flow) of our study region. From within these core areas, we selected 4 grid points that had the strongest relationship with tree growth (NORTH [52.5° N, 115°W], SOUTH [40° N, 120° W], EAST [42.5° N, 95° W], and WEST [47.5° N, 135° W]) for additional analyses. We confirmed that the relationships between radial growth and upper-level flow were stable through time using 24 yr moving-window correlations available in the program DENDROCLIM (Biondi & Waikul 2004). We then used the values of zonal wind at NORTH and SOUTH and meridional wind at EAST and WEST as input variables for a non-rotated principal component analysis (PCA) to capture the variance in 500 hPa flow patterns most closely aligned with radial growth of LALY. From the non-rotated PCA, the first principal component accounted for 57.6% of the variance. We used the factor scores from the first principal component as values for a new variable (hereafter INDEX), representing summertime 500 hPa flow in the western United States. We then used INDEX as the dependent variable in our upper-level flow climate reconstruction (hereafter RINDEX). Because the NARR dataset is limited in temporal resolution (n = 37 yr), we verified the regression model using the leave-one-out (L1O) method. The L1O method is performed by removing a yearly observation (i.e. RINDEX) and running an ordinary least squares (OLS) linear regression. This process is then repeated for every year. Our data started in 1979 and ended in 2015; thus, we produced 37 unique regression models to obtain the predictions used for the reconstruction model validation. We also performed an OLS linear regression without the removal and/or replacement of variables (hereafter FULL). We used the coefficients from the 37 L1O regression models and FULL to calculate the reduction of error (RE) statistic and the RMSE, which are standard metrics used in climatic reconstructions based on tree-ring data (Cook 1985, Gedalof & Smith 2001, Woodhouse & Lukas 2006, Kipfmueller 2008, Fritts 2012, Soulé & Knapp 2019). We also used Pearson correlation values between RINDEX and FULL, L1O, and the raw PCA score (hereafter ACTUAL) as a metric to assess the agreement between variables.

We used a Rodionov regime shift test (Rodionov 2004, Rodionov & Overland 2005) with a 10 yr cutoff length to detect significant ($p < 0.05$, >2 SD) regime shifts to assess the temporal stability of RINDEX. Rodionov (2004) suggests that a shorter cutoff length is more restrictive and requires greater fluctuations in the dataset to produce a statistically significant shift.

To assess the synoptic patterns associated with our reconstruction, we used ESRL 20th Century Reanalysis ver. 2c monthly composites to plot JJA geopotential height anomalies for the top and bottom 5 RINDEX years (1871–2014). To ensure the spatial attributes of the initial flow indices were captured in the reconstruction, we spatially correlated RINDEX with 500 hPa zonal and meridional atmospheric flows and temperature derived from the NCEP–NCAR Reanalysis 1 dataset. We plotted these correlations spatially using KNMI Climate Explorer (Trouet & Oldenborgh 2013).

To investigate the variance in reconstructed 500 hPa flow represented by RINDEX, we calculated the frequency of positive (indicative of ridging) and negative (indicative of troughing) value years within rolling 31 yr windows (1601–2015). We then added a

constant of 10 to RINDEX because both negative (zonal flow east to west or meridional flow north to south) and positive (zonal flow west to east or meridional flow south to north) values were present. Using methodologies outlined by Trouet et al. (2018), we calculated the coefficient of variation (CV) for RINDEX using the same 31 yr moving windows and plotted the temporal patterns. We assessed the trends in the CV values to detect if the variance between ridging and troughing is becoming more or less frequent through time. We also identified extreme years within the moving windows by tabulating the number of years with RINDEX greater than 1 SD from the mean during the associated period.

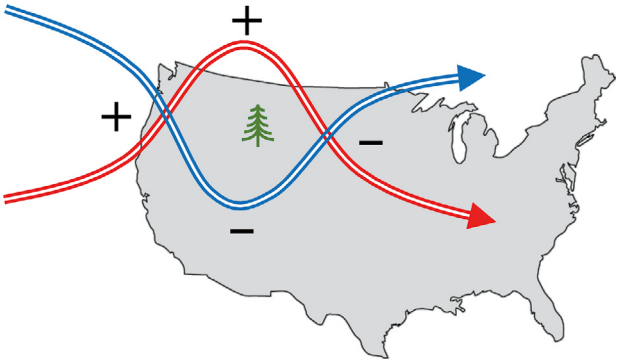

Fig. 2. Direction of relationships between upper-level atmospheric flow and radial tree growth of alpine larch in the Bitterroot National Forest associated with synoptic positioning of 500 hPa flow. The green tree indicates the study location, and the red (ridging) and blue (troughing) lines indicate common synoptic setups in the climatological summer

3. RESULTS

Spatial pattern correlations indicate that radial tree growth increases when meridional and zonal flows are set up in a ridging pattern north and west of the study location. When meridional and zonal flows are synoptically set up in a troughing pattern, negative relationships with tree growth are present (Fig. 2).

The 4 locations that we used for PCA RINDEX had strong relationships to tree growth in the BNF (NORTH: $r = 0.642$, $p < 0.001$; SOUTH: $r = -0.584$, $p < 0.001$; EAST: $r = -0.497$, $p = 0.001$; WEST: $r = 0.504$, $p = 0.001$; Fig. 3). The DENDROCLIM analysis to assess the stability of the relationships reveals signifi-

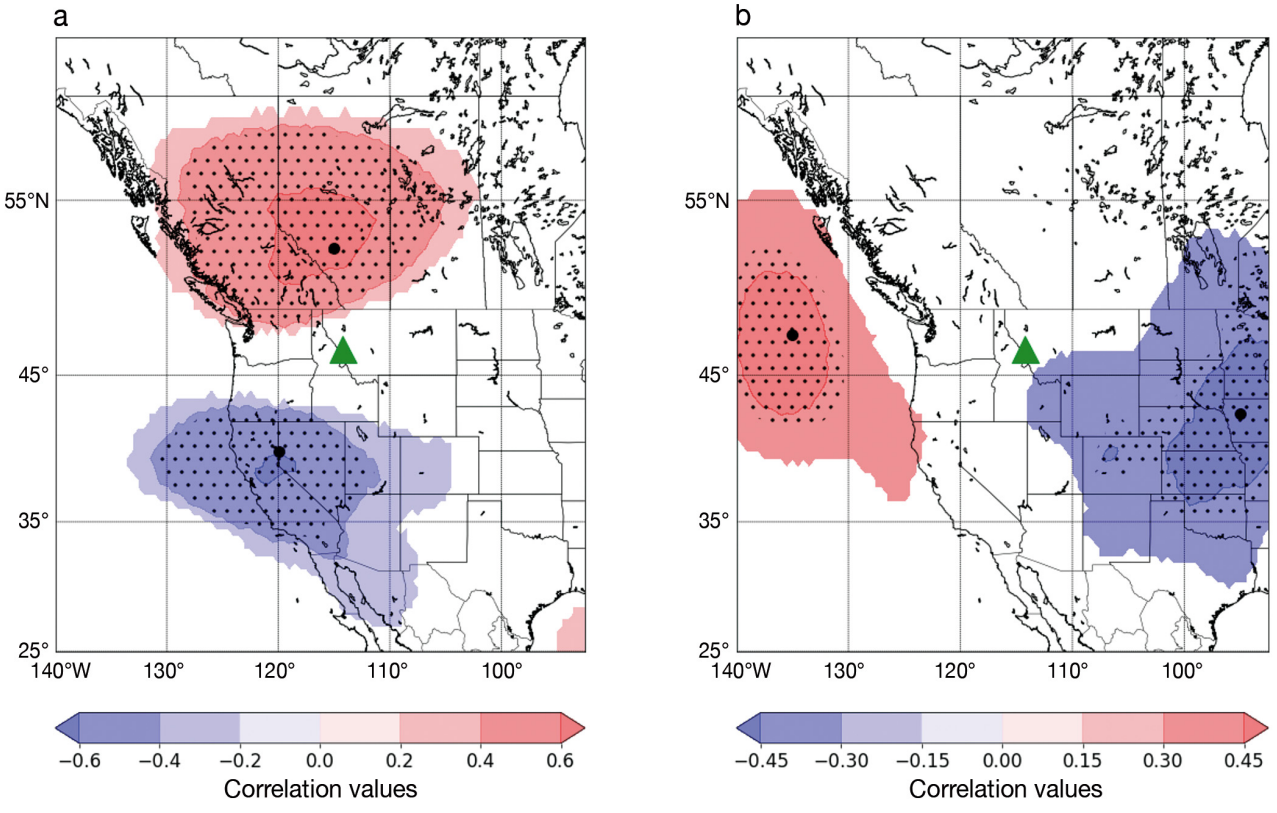

Fig. 3. Spatial relationship (Pearson) between the subset of core samples (COMBO) tree-ring chronology and upper-level (500 hPa) (a) zonal and (b) meridional flows from the North American Regional Reanalysis dataset (1979–2015). Colors indicate r-values, and black gridpoints indicate significance ($p = 0.01$). Large black dots indicate the 4 locations of our principal component analysis climate reconstruction. The green triangle represents the study area. Note differences in correlation value color scales

cant ($p < 0.05$) r-values between 0.4 and 0.5 for north and west and −0.4 and −0.5 for south and east for each 24 yr moving window. Positive RE values, in association with the RMSE values being within 1 SD of the sample mean, confirm the validity of our climate reconstruction (Table 2, Fig. 4; Fritts 2012). Pearson correlation values indicate the instrumental PCA is closely associated with the values produced by the L1O and full linear regression models (Table 2).

Spatial pattern correlations of the geopotential height anomalies associated with the highest and lowest 5 RINDEX summers indicate that high RINDEX values are indicative of synoptic ridging over the western Montana study region (Fig. 5). Summers within the RINDEX that exhibit low flow values are associated with atmospheric troughing. Our RINDEX positively (west and north) and negatively (east and south) spatially correlates to the same regions that were identified between tree growth and the instrumental NARR 500 hPa atmospheric flow in the preliminary phase of the study (Fig. 6).

Over the 120 yr instrumental record, the relationships between RINDEX and surface climatic conditions are significant and have a logical direction (Table 3). For example, positive RINDEX values are indicative of enhanced summertime ridging, leading to higher temperatures, reduced precipitation, and drought conditions that, in turn, are conducive for enhanced wildfire activity.

The temporal pattern of positive and negative years within rolling 31 yr windows shows 5 extended periods dominated by ridging and 5 dominated by troughing (Fig. 7a). During periods of decreasing variance of RINDEX, one flow type (i.e. ridging or troughing) becomes more dominant (Fig. 7). For example, the lowest variance for any 31 yr window was in 1906 (Fig. 7b), and this is concurrent with the highest frequency of troughing (Fig. 7a). Trends in variance are mixed, with significant negative trends for the last 31 yr ($p < 0.05$) and 50 yr ($p < 0.001$) of the record, and for the full reconstruction ($p < 0.001$), but significant ($p < 0.001$) positive trends for the last 100 yr of the record.

Table 2. Verification statistics for the leave-one-out (L1O) and full regression models used to reconstruct upper-level (500 hPa) atmospheric flow in the western United States. The full regression model (Full) includes data from all 37 yr of North American Regional Reanalysis 500 hPa flow data. The L1O technique is based on 37 unique regression models, each 1 run leaving out the corresponding year of data. Actual is the factor scores generated from the principal component analysis. $^{**}p < 0.01$

Statistic	RINDEX
RE (L1O)	0.526
RE (Full)	0.460
RMSE (L1O)	0.715
RMSE (Full)	0.669
Standard Deviation (Actual)	1.000
r-value (Full/L1O)	0.996**
r-value (Actual/Full)	0.734**
r-value (Actual/L1O)	0.689**

4. DISCUSSION

Zonal flow north and south of the study site and meridional flow east and west of the study site have

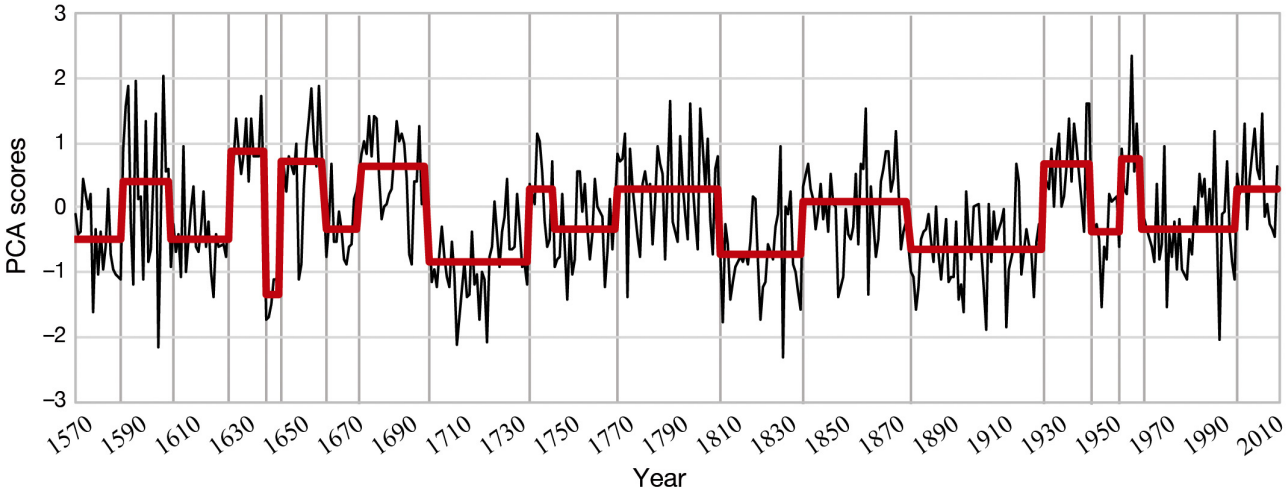

Fig. 4. Climate reconstruction (solid black line) of principal component analysis (PCA) upper-level (500 hPa) atmospheric flow ($m\ s^{-1}$) from 1571 to 2015 using the subset of core samples (COMBO) tree-ring chronology. The red line identifies significant ($p < 0.05$) regime shifts in 500 hPa flow using the Rodionov regime shift test

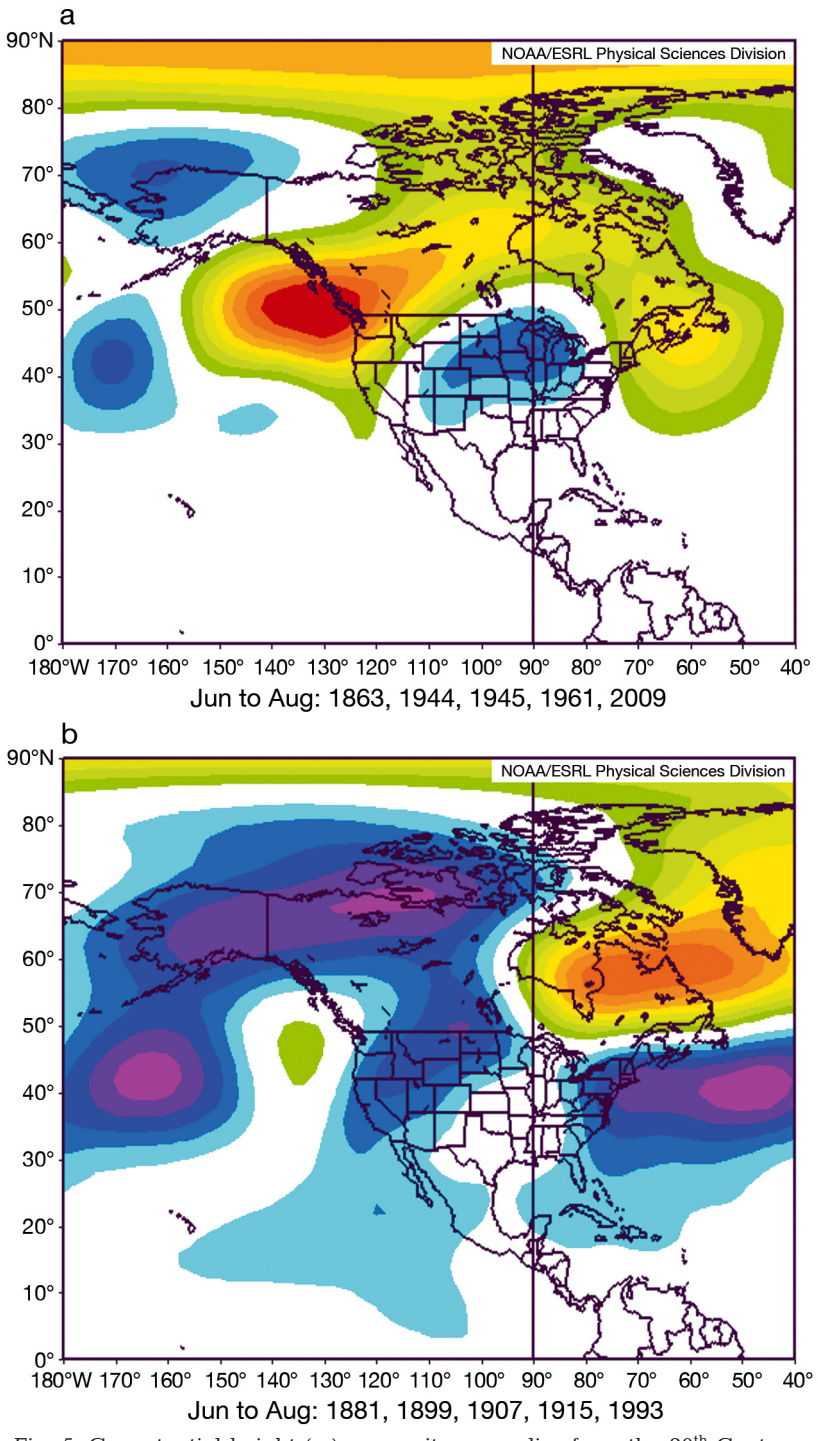

Fig. 5. Geopotential height (m) composite anomalies from the 20th Century Reanalysis ver. 2c dataset plotted with the 10 most extreme ([a] 5 highest and [b] 5 lowest) reconstructed principal component analysis 500 hPa flow years (m s^{-1})

opposite effects on LALY growth. When zonal flow is positive (i.e. west to east) north of the study site and meridional flow is positive (i.e. south to north) west of the study site, tree growth in the BNF tends to be above normal, likely reflecting higher temperatures associated with ridging. When zonal flow is positive south of the study site and meridional flow is positive east of the study site (indicative of troughing), LALY growth in the BNF tends to be below normal. Summers dominated by a troughing pattern allow colder air from Canada to occupy the region, likely causing below-average temperatures and reduced radial growth for LALY (Figs. 2 & 3).

Knapp & Soulé (2017) found that wintertime Arctic sea ice extent is teleconnected to increases in 300 hPa ridging and that these atmospheric conditions are linked to increases in temperature and droughts, leading to increases in wildfire activity. Swain et al. (2014, p 4) found linkages between the major 2013–2014 California drought and the 'ridiculously resistant ridge' (i.e. persistent positive geopotential height) over the Gulf of Alaska (500 hPa). Although the location of the influencing high-pressure system differs geographically from our study, Swain et al. (2014) find linkages between abnormal synoptic-scale atmospheric pressure patterns and extreme weather events.

A shortcoming of PCA is that meaningful values are often reduced to dimensionless variables that can be difficult to interpret. That said, we provide evidence that our PCA RINDEX captures both synoptic ridging and troughing events over the study site throughout the 444 yr reconstructed period. When spatially correlating RINDEX to the NCEP–NCAR Reanalysis 1 dataset (Fig. 6), we find the same spatial patterns that were present when we spatially correlated NARR 500 hPa zonal (Fig. 3a) and meridional (Fig. 3b) flows to tree growth in the BNF (Fig. 6). We corroborated these findings by assessing the dominant synoptic setup during extreme high and low RINDEX years and found that the 5 highest flow years in our reconstructed INDEX exhibit geopotential height anomalies that are emblematic of

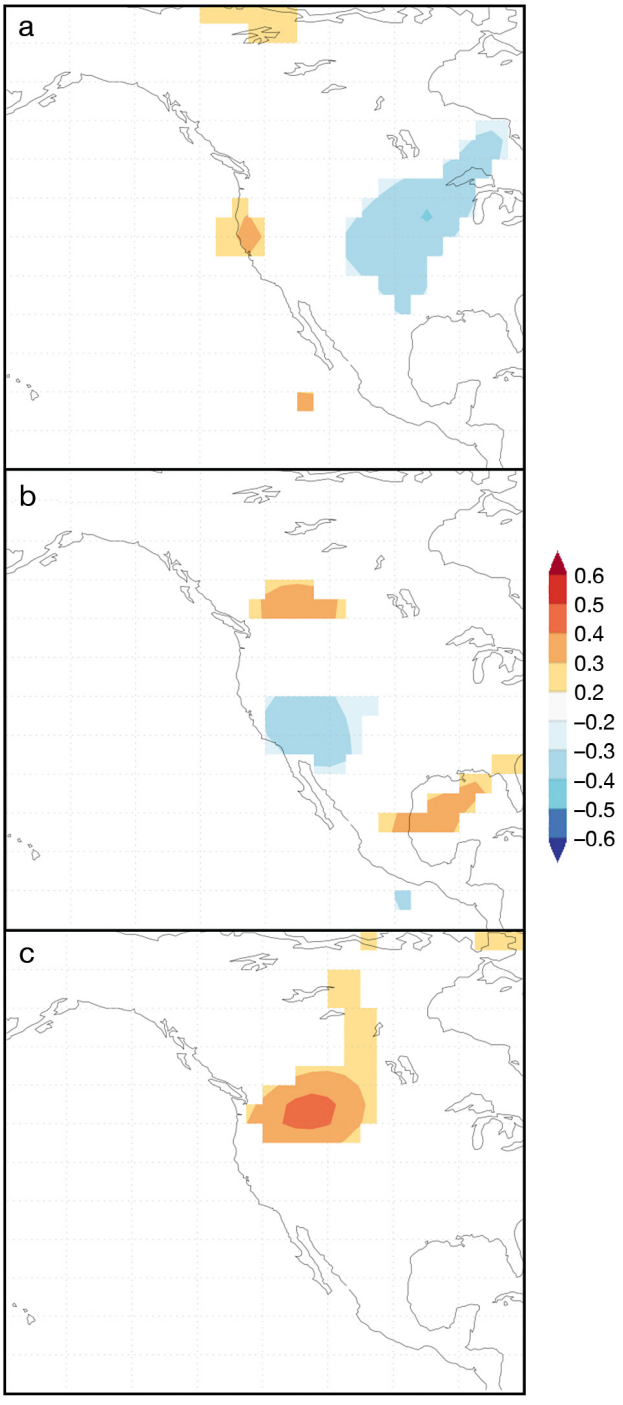

Fig. 6. KNMI Climate Explorer spatial correlation analysis between NCEP–NCAR Reanalysis 1 data (a) 500 hPa meridional flow, (b) 500 hPa zonal wind, and (c) 500 hPa temperature and principal component analysis reconstructed 500 hPa flow (m s^{-1})

a ridging pattern over the study site (Fig. 5a). Inversely, we find that the 5 lowest flow years in the reconstructed INDEX exhibit geopotential height anomalies that are indicative of atmospheric troughing over the study area (Fig. 5b).

Table 3. Relationship (Pearson) between reconstructed upper-level (500 hPa) flow (RINDEX) and climate variables derived from Montana Climate Division 1 (temperature, precipitation, and Palmer Drought Severity Index [PDSI]; 1895–2015). **p < 0.01

Climate variable	RINDEX
Mean temperature (JJA)	0.495**
Maximum temperature (JJA)	0.529**
Minimum temperature (June)	0.326**
Precipitation (JJA)	−0.411**
PDSI (August)	−0.448**

Upper-level atmospheric flow conditions during the reconstructed record (Fig. 4) are not atypical and are similar to Trouet et al. (2018), who found that the current latitudinal positioning of the North Atlantic Jet is not unique to a multi-century period. Trouet et al. (2018) found consistent increases in both the number of anomalous years and the variance of North Atlantic Jet positioning post-1960, but we found that the number of years dominated by summertime ridging or troughing over western North America since the 1960s is generally near the long-term mean, and the variance of RINDEX has been low since the late 1980s (Fig. 7b). However, the Rodionov test suggests a new regime has emerged since 2000 (Fig. 4), and the frequency of ridging years shows that ridging has become more dominant since the early 2000s (Fig. 7a). We also identify a significant decrease in variance between ridging and troughing within the last 50 yr. A decrease in variance, in conjunction with the emergence of a positive shift in an atmospheric flow regime, indicates that ridging could become the dominant pattern over the western United States.

Christiansen & Ljungqvist (2012) identified AD 1800–1899 as a period of pronounced cooling in the western United States in association with the Little Ice Age, and our reconstructions concur. Approximately two-thirds of the years (n = 67) in the 19th century record are below average (i.e. fall below zero in the RINDEX), suggesting enhanced troughing conditions that would co-occur with colder summer conditions in western North America. Further, 2 extended regimes with enhanced troughing occurred from 1809 to 1840 and from 1879 to 1929 including multiple years where the RINDEX exceeds 1 SD below normal (Fig. 4).

The reconstructed upper-level flow patterns agree with individual years and/or decades, with significant climate anomalies including 1910, the 1930s,

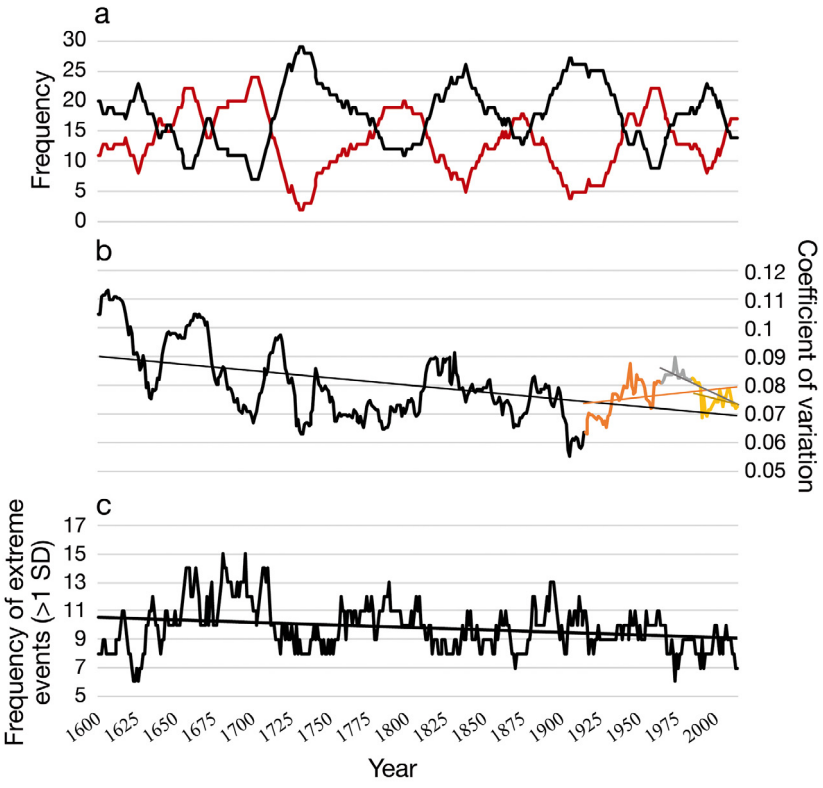

Fig. 7. Rolling 31 yr window analysis for (a) frequency of ridging (red; positive) and troughing (black; negative) events; (b) coefficient of variation (SD mean^{-1}) for the complete record (black line), the last 100 yr (orange line), the last 50 yr (gray line), and the last 31 yr (yellow line); and (c) frequency of extreme (>1 SD) flow years from the principal component analysis 500 hPa upper-level flow climate reconstruction. Linear dark lines indicate the overall trend in the data during the reconstructed period

1961, and 1993 (Fig. 8). Summer 1910 in the western United States was marked by below-average precipitation (Fig. 8d,e) in association with an early snowmelt, leading to soil moisture and fuel conditions typical of late September in early August (Chapman 1910, Egan 2009). These conditions, in association with strong winds, contributed to what is commonly referred to as the Big Burn, which was a 2 d period in August 1910 when approximately 1.2 million ha burned in northeastern Washington, northern Idaho, and western Montana, resulting in one of the largest forest fires in United States history (Egan 2009, US Forest Service n.d.). The instrumental record (Fig. 8b–e) confirms Chapman's observations of low precipitation and a high drought index. Enhanced ridging leading to drought conditions (August Palmer Drought Severity Index [PDSI] = –2.7), concurrent with high surface winds, contributed to the Big Burn of 1910 in the western United States. While the ridging observed in 1910 was not of the same magnitude as that observed in 1961, extreme weather events in 1910 resulted in more damage to the built environment and high loss of human life (Egan 2009).

Drought conditions (PDSI < –1) in western Montana occurred during 1929–1940, with August PDSI values for Montana Climate Division 1 averaging –2.74 (Fig. 8d). Concurrent with the extended drought, our RINDEX suggests this period was dominated by ridging, as our reconstruction indicates above-average PCA values for each year of the drought period. Four years in the 1930s had PCA values exceeding 1 SD for RINDEX within a ridging regime that extended from 1928 to 1945 (Fig. 4). Thus, by various metrics, an extended period of summertime ridging was concurrent with the 1930s drought.

Summer 1993 was the coldest on record for Montana Climate Division 1 (National Climatic Data Center 2016). From summer 1992 to summer 1993, there was a dramatic switch from a ridging to troughing pattern (positive PCA value to negative PCA value; Fig. 8a). This troughing pattern during 1993 led to anomalously low mean, maximum, and minimum temperatures and above-normal precipitation and PDSI values. The summer troughing pattern that contributed rain and cool conditions to the region coincided with a below-average (79.7%) wildfire year during 1933 (Federal Fire Occurrence 2016). Likewise, the anomalous ridging of 1961 (Fig. 8) coincided with high summer mean, maximum, and minimum temperatures and below-average precipitation, leading to drought conditions (National Climatic Data Center 2016).

While our study provides strong evidence that (1) atmospheric ridging has become the dominant synoptic setup and (2) there has been an overall decrease in variance of upper-level patterns, we acknowledge limitations and the need for further investigation into this area of tree-ring science. The most notable limitation of the study is the use of PCA as a tool to reduce the number of variables in our climate reconstruction. While we did provide evidence that positive PCA values were indicative of ridging and negative PCA values were indicative of troughing, there is still uncertainty when interpreting these dimensionless values.

Sustained changes in upper-level atmospheric flow can contribute to prolonged and devastating climatic

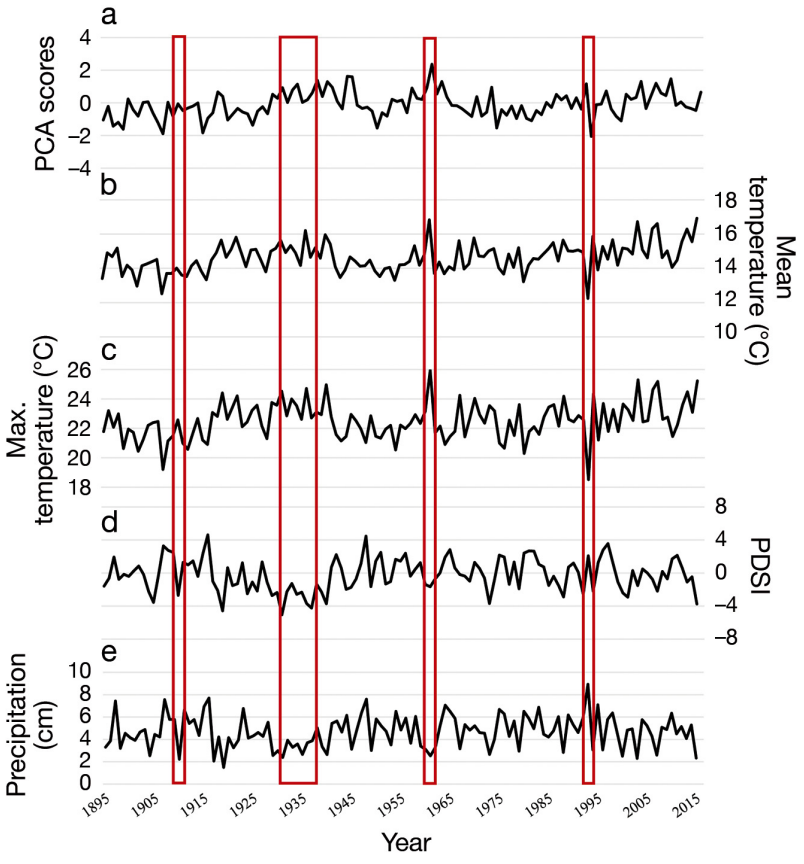

Fig. 8. Temporal pattern (1895–2015) of (a) principal component analysis (PCA) reconstructed 500 hPa flow (m s^{-1}), (b) Montana Climate Division 1 mean summer (JJA) temperature (°C), (c) Montana Climate Division 1 maximum summer (JJA) temperature (°C), (d) Montana Climate Division 1 Palmer Drought Severity Index (PDSI; August), and (e) Montana Climate Division 1 total summer (JJA) precipitation (cm). Red rectangles indicate 1910, the 1930s, 1961, and 1993

events in the mid-latitudes (e.g. wildfires, floods, heat waves). We recognize the need for further research in this area and urge the scientific community to investigate modes in which tree rings can be used as a proxy to understand these changes. One avenue of research that we believe would be beneficial is increasing the numbers of tree species and study locations as well as spatial coverage. Increasing these attributes would lead to a more robust assessment of changes in upper-level patterns and could potentially eliminate the need for PCA and allow reconstruction of full synoptic-scale atmosphere circulation patterns via climate field reconstruction methods.

5. CONCLUSIONS

Recent research suggests that observed shifts in upper-level flow are occurring in the summer due to reductions in Arctic sea ice, which leads to extreme weather events such as heat waves and droughts (Meehl & Tebaldi 2004, Tang et al. 2014, Cvijanovic et al. 2017, Vavrus et al. 2017). Here, we investigated a spatial relationship between LALY radial growth in the BNF and upper-level (500 hPa) zonal and meridional flows. Specifically, we found that zonal flow north and meridional flow west of our tree-ring study sites positively impact radial tree growth, as these conditions are conducive to upper-level ridging causing above-average temperatures that promote radial growth of high-elevation conifers. Conversely, zonal flow south and meridional flow east of our study sites promote troughing, colder summer temperatures, and decreased LALY radial growth. Given the strength of these relationships, we were able to develop a tree-ring-based proxy reconstruction of 500 hPa over western North America for the period AD 1571–2015. Over this 444 yr period, we identified multiple decades-long regimes dominated by either enhanced ridging or troughing.

We found that variance between ridging and troughing and the frequency of either extreme ridging or troughing years have decreased since approximately 1973. Thus, our PCA reconstruction of 500 hPa flow suggests that shifts between ridging and troughing patterns are decreasing over western North America during the summer months. However, our regime shift analysis (Fig. 4) and ridging–troughing frequency analysis (Fig. 7a) both indicate that a new ridging regime has emerged since the early 2000s. Years of extreme ridging are concurrent with increased temperature and decreased precipitation (i.e. drought). Vavrus et al. (2017) predict that increased ridging over North America will persist into AD 2100, with the greatest increases between 40° and 45° N, which is near the latitude of our study sites. If ridging continues to increase, in conjunction with reduced variance of ridging and troughing, heat-related extreme weather events will continue to become more common and likely will affect wildfire activity and water resources.

Acknowledgements. We would like to thank Heather Guy for her help in developing Python scripts used in this study. Thank you to Justin Maxwell and J. Stephen Shelly for assistance with fieldwork. Logistical support was provided by the United States Forest Service.

LITERATURE CITED

Arno SF, Habeck JR (1972) Ecology of alpine larch (*Larix lyallii* Parl.) in the Pacific Northwest. Ecol Monogr 42: 417–450

Barnes EA, Screen JA (2015) The impact of Arctic warming on the mid-latitude jet stream: Can it? Has it? Will it? Wiley Interdiscip Rev Clim Change 6:277–286

Biondi F, Waikul K (2004) DENDROCLIM2002: a C++ program for statistical calibration of climate signals in tree-ring chronologies. Comput Geosci 30:303–311

Brewer MC, Mass CF (2016) Projected changes in heat extremes and associated synoptic-and mesoscale conditions over the Northwest United States. J Clim 29:6383–6400

Casty C, Handorf D, Raible CC, González-Rouco JF and others (2005) Recurrent climate winter regimes in reconstructed and modelled 500 hPa geopotential height fields over the North Atlantic/European sector 1659–1990. Clim Dyn 24:809–822

Chapman HH (1910) Fires on the Flathead Forest in Montana. Am For 16:657–658

Christiansen B, Ljungqvist FC (2012) The extra-tropical Northern Hemisphere temperature in the last two millennia: reconstructions of low-frequency variability. Clim Past 8:765–786

Cohen J, Screen JA, Furtado JC, Barlow M and others (2014) Recent Arctic amplification and extreme mid-latitude weather. Nat Geosci 7:627–637

Cook ER (1985) A time series analysis approach to tree-ring standardization. PhD dissertation, University of Arizona, Tucson, AZ

Cvijanovic I, Santer BD, Bonfils C, Lucas DD, Chiang JCH, Zimmerman S (2017) Future loss of Arctic sea-ice cover could drive a substantial decrease in California's rainfall. Nat Commun 8:1947

Egan T (2009) The Big Burn: Teddy Roosevelt and the fire that saved America. Houghton Mifflin Harcourt, Boston, MA

Francis JA (2017) Why are Arctic linkages to extreme weather still up in the air? Bull Am Meteorol Soc 98: 2551–2557

Francis JA, Vavrus SJ (2012) Evidence linking Arctic amplification to extreme weather in mid-latitudes. Geophys Res Lett 39:L06801

Fritts HC (2012) Tree rings and climate. Elsevier, London

Gedalof Z, Smith DJ (2001) Interdecadal climate variability and regime scale shifts in Pacific North America. Geophys Res Lett 28:1515–1518

Graumlich LJ, Brubaker LB (1986) Reconstruction of annual temperatures (1590–1979) for Longmire, Washington, derived from tree rings. Quat Res 25:223–234

Holmes RL (1983) Computer-assisted quality control in tree-ring dating and measurement. Tree-Ring Bull 43:69–78

Kipfmueller KF (2008) Reconstructed summer temperature in the northern Rocky Mountain wilderness, USA. Quat Res 70:173–187

Knapp PA, Soulé PT (2017) Spatio-temporal linkages between declining Arctic sea-ice extent and increasing wildfire activity in the western United States. Forests 8:313

Meehl GA, Tebaldi C (2004) More intense, more frequent, and longer lasting heat waves in the 21st century. Science 305:994–997

Mesinger F, DiMego G, Kalnay E, Mitchell K and others (2006) North American regional reanalysis. Bull Am Meteorol Soc 87:343–360

Montpellier EE, Soulé PT, Knapp PA, Shelly JS (2018) Divergent growth rates of alpine larch trees (*Larix lyallii* Parl.) in response to microenvironmental variability. Arct Antarct Alp Res 50:e1415626

National Climatic Data Center (2016) US national/state/divisional data. http://www7.ncdc.noaa.gov/CDO/CDODivisionalSelect.jsp (accessed 12 August 2018)

Nichols H, Kelly PM, Andrews JT (1978) Holocene palaeowind evidence from palynology in Baffin Island. Nature 273:140–142

Peterson DW, Peterson DL (1994) Effects of climate on radial growth of subalpine conifers in the northern Cascade Mountains. Can J Res 24:1921–1932

Porter DF, Cassano JJ, Serreze MC (2012) Local and large-scale atmospheric responses to reduced Arctic sea ice and ocean warming in the WRF model. Geophys Res Lett 117:D11115

Regent Instruments (2011) WinDENDRO: an image analysis system for tree-rings analysis. Regent Instruments, Quebec

Rodionov SN (2004) A sequential algorithm for testing climate regime shifts. Geophys Res Lett 31:L09204

Rodionov SN, Overland JE (2005) Application of a sequential regime shift detection method to the Bering Sea ecosystem. ICES J Mar Sci 62:328–332

Screen JA, Simmonds I (2013) Exploring links between Arctic amplification and mid latitude weather. Geophys Res Lett 40:959–964

Screen JA, Simmonds I (2014) Amplified mid-latitude planetary waves favour particular regional weather extremes. Nat Clim Chang 4:704–709

Seim A, Schultz JA, Beck C, Bräuning A and others (2018) Evaluation of tree growth relevant atmospheric circulation patterns for geopotential height field reconstructions for Asia. J Clim 31:4391–4401

Soulé PT, Knapp PA (2019) A 400-year reconstruction of wintertime Arctic sea-ice extent using a high-elevation, mid-latitude tree-ring record. Int J Biometeorol 63: 1217–1229

Stokes MA, Smiley TL (1996) An introduction to tree-ring dating. University of Arizona Press, Tucson, AZ

Swain DL, Tsiang M, Haugen M, Singh D, Charland A, Rajaratnam B, Diffenbaugh NS (2014) The extraordinary California drought of 2013/2014: character, context, and the role of climate change. Bull Am Meteorol Soc 95: S3–S7

Tang Q, Zhang X, Francis JA (2014) Extreme summer weather in northern mid-latitudes linked to a vanishing cryosphere. Nat Clim Chang 4:45–50

Trouet V, Van Oldenborgh GJ (2013) KNMI Climate Explorer: a web-based research tool for high-resolution paleoclimatology. Tree-ring Res 69:3–13

Trouet V, Babst F, Meko M (2018) Recent enhanced high-summer North Atlantic Jet variability emerges from three-century context. Nat Commun 9:180

USGS (2016) Federal Fire Occurence https://wildfire.cr.usgs.gov/firehistory/data.html (accessed 20 August 2018)

US Forest Service (n.d.) The Great Fire of 1910. https://www.fs.usda.gov/Internet/FSE_DOCUMENTS/stelprdb5444731.pdf (accessed 14 September 2018)

Vavrus SJ, Wang F, Martin JE, Francis JA, Peings Y, Cattiaux J (2017) Changes in North American atmospheric circulation and extreme weather: influence of Arctic amplification and Northern Hemisphere snow cover. J Clim 30:4317–4333

Wigley TML, Briffa KR, Jones PD (1984) On the average of correlated time series, with applications in dendroclimatology and hydrometeorology. J Clim Appl Meteorol 23:201–213

Wise EK, Dannenberg MP (2014) Persistence of pressure patterns over North America and the North Pacific since AD 1500. Nat Commun 5:4912

Wise EK, Dannenberg MP (2017) Reconstructed storm tracks reveal three centuries of changing moisture delivery to North America. Sci Adv 3:e1602263

Woodhouse CA, Lukas JJ (2006) Multi-century tree-ring reconstructions of Colorado streamflow for water resource planning. Clim Change 78:293–315

Wu Y, Smith KL (2016) Response of Northern Hemisphere midlatitude circulation to Arctic amplification in a simple atmospheric general circulation model. J Clim 29: 2041–2058

Editorial responsibility: Guoyu Ren, Beijing, PR China

Submitted: January 29, 2019; Accepted: February 10, 2020
Proofs received from author(s): March 12, 2020